Modelling the effect of climate change on nutrient loading, temperature regime and algal biomass in the Gulf of Finland

Arto Inkala[1], Ämer Bilaletdin[2] and Victor Podsetchine[2]

[1] *The Environmental Impact Assessment Center of Finland, Tekniikantie 17, FIN-02150 Espoo, Finland*
[2] *Regional Environmental Agency of Häme, P.O. Box 297, FIN-33101 Tampere, Finland*

Climate changes and the potential related warming can change runoff, nutrient transport, mean wind velocities and water temperatures. These changes will further affect algal growth in a way that can be modelled. The changes to the nutrient load, temperature regime and algal biomass were simulated by three separate models. The simulations were made for the years 2020, 2050 and 2090. The simulated temperature variations and nutrient loading dynamics were used by algal model to predict changes of the algal biomass under the three different climate scenarios. According to the different scenarios, the maximum temperature of the surface water increased by 0.3–6.2 °C, but in the deeper waters (> 40 m) by less than 0.1 °C. The major part of the nutrient loads is anthropogenic and this part did not change in the scenarios. Thus, the changes in the algal biomass were also relatively small. However, the timing and quantity of spring bloom did change noticeably, at most in 2090, two weeks earlier and 20% higher than nowadays.

Introduction

The assessments of the effect of climate change are based nowadays on the results of mathematical models. During the last forty years, numerical models have proved to be useful research tools in environmental studies. The first water system model was developed by Hansen (1956). More than hundred models and almost thousand case studies have been investigated before the 1990s (Koponen *et al*. 1992).

The aim of this study is to assess the possible effects of climate changes in the Gulf of Finland. Future climate scenarios, used by temperature and catchment models, were simulated by the stochastic weather generator CLIGEN. CLIGEN has been developed to produce daily meteorological data over the territory of Finland (Carter *et al*. 1995). The changes in the vertical distribution of water temperature were simulated with the one-dimensional vertical PROBE model (Svensson 1978). The effect of
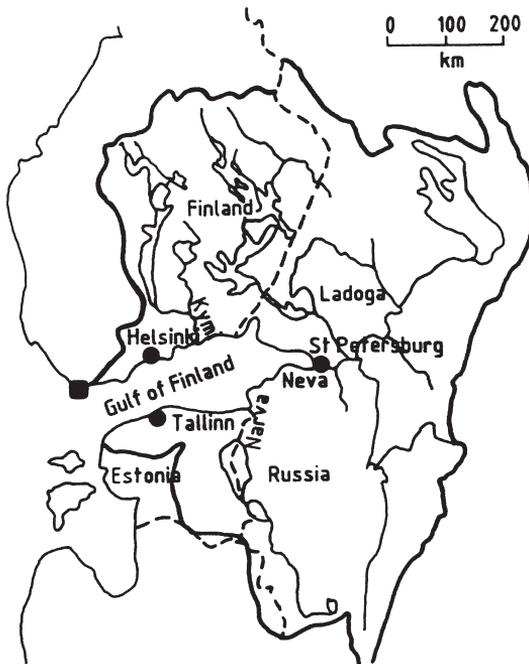
Fig. 1. Drainage basin of the Gulf of Finland. The square marks the location of meteorological stations Russärö and Hanko.

Study site

The drainage basin of the Gulf of Finland is 410 960 km^2. In this study the drainage basin has been divided into four sub-basins: River Kymijoki basin, the basin of rest of Finland, the basin of Russia and the basin of north coast of Estonia. The drainage basin of eastern Finland has been included in the drainage basin of Russia (Table 1, Fig. 1).

The Finnish drainage basin is characterized by a large number of lakes and rivers. The land is dominated by forests (51%), wetlands (27%) and lakes (10%). Agricultural areas (7%) are located in the south-western Finland. The Finnish surface waters are basically oligotrophic. Many lakes form long water systems with slow water exchange. Therefore, the pollution load is mixed in the water systems before it reaches the Baltic Sea. In most of the Finnish coastal rivers the discharge is small. They are characterized by great variations in flow and water quality. The variations can, e.g., be caused by changes in the natural conditions, land use or wastewater loading (HELCOM 1993).

The catchment area of the Gulf of Finland within the borders of Russia is 276 100 km^2 with 80% (215 600 km^2) of the area drained by the river Neva. The total population of the drainage area in Russia is 8.3 million inhabitants, 80% of them living in the St. Peterburg district. The catchment area is low and swampy. In Lake Ladoga the retention time is several weeks so that a significant part of pollutants accumulates in Lake Ladoga (HELCOM 1993).

The drainage basin of the Gulf of Finland covers 26 400 km^2 in Estonia and is populated by 1.27 million inhabitants. On average, 30% of the catchment area consists of arable land, 39% are covered by forests and 20% by swamps. The main

changes on the nutrient loads was calculated by the catchment model of Bilaletdin *et al.* (1996). These results were used as an input to the algal biomass model (Inkala 1993) coupled with a 3-dimensional hydrodynamic model (Kokkila 1995).

In large or complex model applications the available measurement data are often insufficient. So typical dynamics of temperature profiles and algal biomass concentrations were also used as verification criteria in this investigation. All models were calibrated using the weather conditions of the year 1992.

Table 1. Some characteristics of the subcatchments of the Gulf of Finland. A = area, p_l = lake percentage, p_f = field percentage, Mq = mean runoff.

Subcatchment	A (km^{-2})	p_l (%)	p_f (%)	Mq (ls^{-1} km^{-2})
River Kymijoki	37 200[1]	17.3[3]	6.3[3]	7.7[1]
Rest of Finland	9 700[1]	3.2[3]	26.2[3]	9.1[1]
Russia	337 660[1][2]	17.0[2]	10.9[2]	7.5[2]
Estonia	26 400[2]	6.2[2]	30.0[2]	11.8[2]

[1]Leppäjärvi (1992), [2]HELCOM (1993), [3]EDS (environmental data system of the Finnish Environment Institute).

river is the River Narva. About 39 000 km² (70%) of the watershed of the River Narva belong to Russia (HELCOM 1993).

The area of the Gulf of Finland itself is approximately 30 000 km² and its mean depth is less than 40 m (Merenkulkuhallitus 1992, Kokkila 1995). The greatest part of the fresh water comes from the River Neva (about 76% of river water (Ehlin 1981)). Thus, the salinity increases from east to west. It is about 2–6‰ in surface water and about 5–9‰ in the deep water (Kullenberg 1981). The Estonian coastal area is steep unlike the Finnish one. The Gulf of Finland is stratified during summer (Pitkänen *et al.* 1990, 1993).

Material and methods

The catchment model

The loading data is given in Tables 2 and 3. The catchment model consists of two components: a runoff model (HBV) and a nutrient transport model. The structure of the catchment model is described more thoroughly by Bilaletdin *et al.* (1996). The HBV runoff model is a relatively simple conceptual model, originally developed by Bergström (1976). A modification of the HBV model (Vehviläinen 1992) was used. The model has a number of independent parameters, of which values must be found by calibration. There are also parameters describing characteristics of the basin and climate, which are kept constant during model calibration. Normally the catchment area is divided into several sub-catchments. It is also possible to separate the contributions of forested and agricultural areas. The following input data are needed: precipitation, temperature and evaporation from all local stations. As output data of the model the following quantities are produced: discharges, soil moisture and soil frost.

Total phosphorus and nitrogen transport was calculated separately for forested and agricultural areas in the catchment as the product of runoff by concentration (1):

$$L = Q_{fo} \times c_{fo} + Q_{ag} \times c_{ag} \qquad (1)$$

where L = transport (kg s^{-1}), Q = discharge (m^3 s^{-1}),

Table 2. The phosphorus mass flows (t a^{-1}) of diffuse loading (L_{diff}), point source loading (L_{point}) and total loading (L_{tot}).

Subcatchment	L_{diff} (t a^{-1})	L_{diff} (kg km^{-2} a^{-1})	L_{point} (t a^{-1})	L_{tot} (t a^{-1})
River Kymijoki	216[1,2,3]	6	94[1,2,3]	310
Rest of Finland	256[1,2]	26	38[1,2]	294
coast			158[1,2]	158
Russia	960[1,4]	3	7 863[1]	8 823
Estonia	351[1]	13	1 666[1]	2 017
Sum	1 783		9 819	11 602

[1]HELCOM (1993), [2]HELCOM (1991), [3]Heinonen (1993), [4]Lääne *et al.* (1991).

Table 3. The nitrogen mass flows (t a^{-1}) of diffuse loading (L_{diff}), point source loading (L_{point}) and total loading (L_{tot}).

Subcatchment	L_{diff} (t a^{-1})	L_{diff} (kg km^{-2} a^{-1})	L_{point} (t a^{-1})	L_{tot} (t a^{-1})
River Kymijoki	6 295[1,2,3]	169	1 005[1,2,3]	7 300
Rest of Finland	9 143[1,2]	943	817[1,2]	9 960
coast			4 794[1,2]	4 794
Russia	26 040[1,4]	77	125 550[1]	151 590
Estonia	7 377[1]	279	29 398[1]	36 775
Sum	48 855		161 564	210 419

[1]HELCOM (1993), [2]HELCOM (1991), [3]Heinonen (1993), [4]Lääne *et al.* (1991).
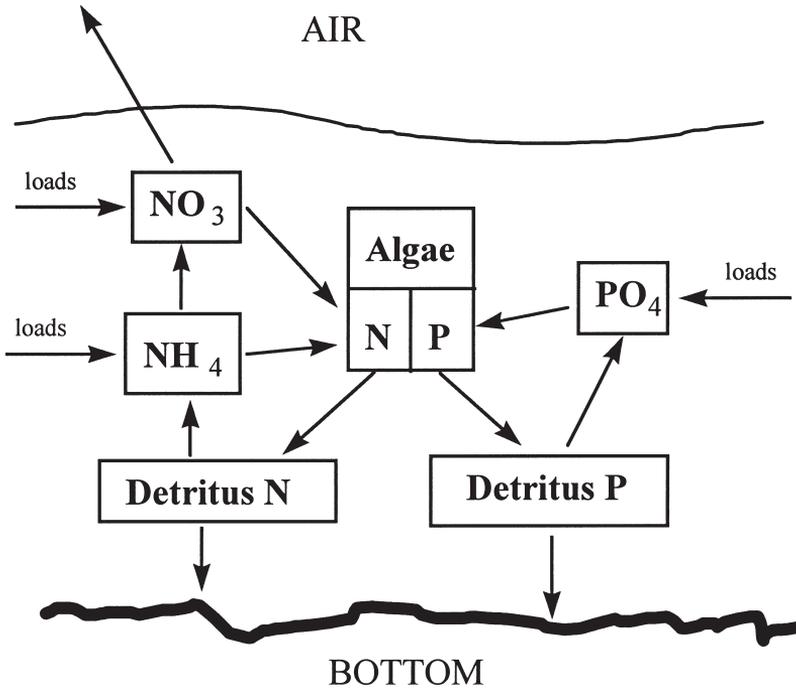
Fig. 2. Flow diagram of the algal model.

c = concentration (kg m^{-3})

Nutrient concentration equations (2, 3) for forest and agricultural areas are the following:

$c_{fo} = c_{0fo} \times f_{lp}$(lake percentage) $\times f_{ca}$(catchment area) $\times f_{ru}$(runoff) $\times f_{sf}$(soil frost) (2)

$c_{ag} = c_{0ag} \times f_{lp}$(lake percentage) $\times f_{ca}$(catchment area) $\times f_{ru}$(runoff) $\times f_{sf}$(soil frost) $\times f_{ct}$(cover type) (3)

The principle of the equation is that the standard concentrations (c_{0fo}, c_{0ag}), referring to a certain standard catchment and standard hydrological situation for forest and agricultural areas, are corrected using empirical functions (f_{lp}(lake pecentage), ...) (Bilaletdin *et al*. 1996). The functions are designed so that their value is equal to one in the standard situation. The dynamical runoff calibration was made by using the discharges of River Kymijoki. The simulated runoff values of River Kymijoki were also used in the different sub-catchments. Due to the lack of dynamical data, the nutrient transport calibration was made by using the annual transport values.

In the catchment model, the present values and scenarios for the years 2020, 2050 and 2100 have been used (Bilaletdin *et al*. 1996). The discharges for forested and agricultural areas were calculated using the HBV runoff model. The assessed discharge and soil frost values were used in the nutrient transport model. The nutrient transport values of the sub-catchments of the Gulf of Finland were summed together. Comparing the annual runoff and transport values of future time horizon (2020, 2050, 2100) with the values of present time we can get the annual effect of climate change.

It is possible to estimate the bioavailable proportion of total nutrient. For instance 30% (Ekholm 1991) of diffuse phosphorus transport is assumed to be available dissolved reactive phosphorus (DRP) and 100% of point source loading. Correspondingly, the same values for dissolved reactive nitrogen (DRN) and total nitrogen were estimated to be 40% and 100%. The amount of DRN depends strongly on the percentage of cultivated land (Rekolainen *et al*. 1991).

The temperature model

A one-dimensional non-steady lake-averaged hydrodynamic model, PROBE originally developed by Svensson (1978), was used for calculation of water temperature variations in the Gulf of Finland. The western boundary of the Gulf is close to the longitude 23° and there are about 30 layers in the model.

The model includes momentum and energy conservation equations. The turbulence part of the model is based on the k-ε theory. It calculates temporal and vertical changes of water temperature, horizontal components of velocity and turbulent exchange coefficients. The model uses as input data basic meteorological parameters, such as air temperature, wind speed, humidity and cloudiness for the computation of the boundary fluxes at the air-water interface.

The algal model

The algal model is coupled with the 3-dimensional hydrodynamic model. The Gulf of Finland was divided into a grid with resolution of five kilometers. There is ten vertical layers. Bathymetric data were obtained from the sea maps (Merenkulkuhallitus 1992). The western boundary is the same as in the temperature model.

The algal model does not calculate the temperature. The values of temperature in the different layers were taken from the result of the temperature model. The thermocline depth in the temperature and hydrodynamic model were at the same depth layer.

The model simulates nitrogen in four forms: ammonium, nitrate, the intracellular nitrogen of phytoplankton and nitrogen in detritus. Phosphorus was modeled in three forms: phosphate, the intracellular phosphorus of phytoplankton and phosphorus in detritus. All phytoplankton species were included into one simulated variable. The flow diagram of the model is given in Fig. 2. The variables, parameters and the equations are presented in Apps. 1–4.

Detritus nitrogen (App. 3: eq. 1) is formed from phytoplankton intracellular nitrogen (c_{NA}), when phytoplankton dies, settles onto the bottom or is predated by zooplankton. Intracellular nitrogen is released immediately after the decay of algae (M_A). The detritus nitrogen changes to ammonium (b_0) while the detritus sinks (n_{Ndet}).

Ammonium (App. 3: eq. 2) comes from atmospheric and riverine load and via the decay of detritus nitrogen. The release from the sediment is zero in this application, because the accumulation of nitrogen into the bottom sediment and denitrification cancels the influence (Pitkänen

1994). Ammonium is nitrified at first to nitrite and then to nitrate by bacteria. The nitrification rate (β_1) is assumed to be constant. Different phytoplankton species prefer either ammonium or nitrate as their nutrient (App. 3: eqs. 13 and 14). In the model this is taken into account by the preference coefficient (a_{pr}), which determines the uptake rate of nitrate and ammonium for different species (Scavia *et al.* 1976). The sedimentation rate of ammonium is zero.

Nitrite is assumed to decay so rapidly to nitrate that it is not simulated in the model. The nitrate load comes from rivers and the atmosphere. Denitrification takes place near the bottom sediment. The nitrate uptake of phytoplankton is simulated similarly as ammonium (App. 3: eqs. 3, 14 and 15).

The cycle of bioavailable phosphorus (App. 3: eqs. 4, 5 and 7) is described in a similar way as bioavailable nitrogen. If dissolved nitrogen (nitrate and ammonium) is considered as one simulation variable, we get the phosphorus equations by replacing nitrogen (N) in the nitrogen equations (App. 3: eqs. 1, 2, 3 and 6) with phosphorus (P). Of course the parameter values are different. The decay rate of phosphate (denitrification) is zero, so this term is not included in the eq. 5 (App. 3).

The growth of phytoplankton (App. 3: eq. 9) depends on temperature (App. 3: eqs. 18 and 19) (Frisk and Nyholm 1980) and intracellular nutrient concentration (App. 3: eq. 17) (Jrgensen 1988). Nutrient uptake depends on concentration in water, intracellular concentrations and also temperature (App. 3: eqs. 15, 16, 18 and 19). The dependence on intracellular concentration is linear and that on the concentration in water follows the Michaelis-Menten formula. The effect of light attenuation on growth is taken into account in two ways. There is a maximal growth rate in the surface layer (depth 0–12 m). The growth rate decreases linearly to the depth of 20 m and is zero below. The seasonal changes are taken into account through a very simple linear light limiting factor (App. 3: eqs. 20 and 21). It is also assumed that intense light does not limit the growth.

The decay (respiration, mortality, grazing, sedimentation) rate of phytoplankton depends on temperature (App. 3: eqs. 18 and 19). The phytoplankton concentrations decrease very fast after the spring bloom, when the nutrients run out. In
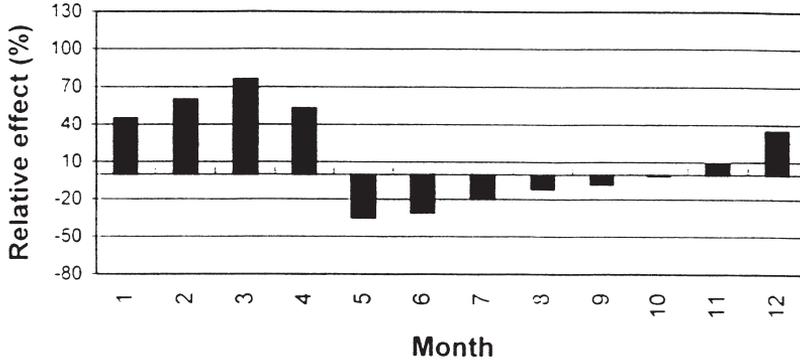
Fig. 3. Monthly effects of climate change (Carter *et al.* 1995) on nitrogen transport in the catchment area of the Gulf of Finland.
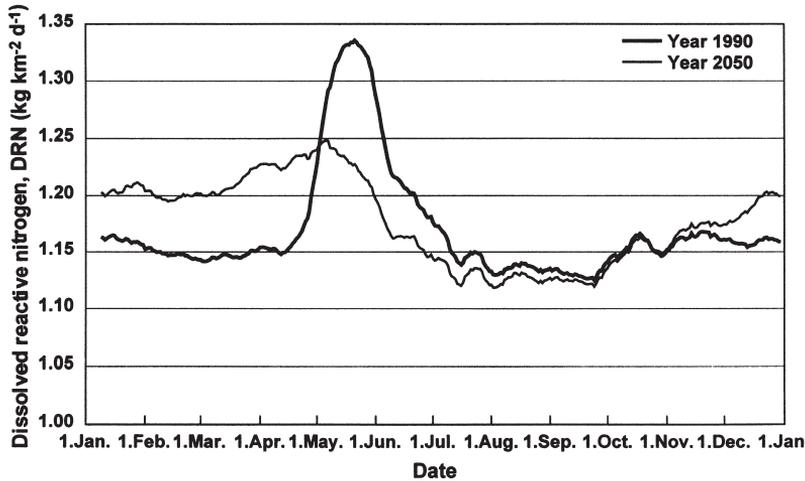
Fig. 4. The effect of climate change (Carter *et al.* 1995) on dissolved reactive nitrogen transport (diffuse and point source loading) in the drainage basin of the Gulf of Finland. A bold line is the present time and a regular line is year 2050.

the model, fast sedimentation (S_{fa}) depends on the intracellular nutrients of phytoplankton. It begins when the concentration of the intracellular nutrients (characteristic quantity App. 3: eq. 17) decreases below the critical value (FL). A vertical mean value is used because now the sedimentation occurs at the same time at all depths.

Results

Catchment model

The calibration results for the sub-catchments of the Gulf of Finland are distributed logically (Table 4). In the calibration, the standard concentrations of phosphorus and nitrogen in the different parts of

Table 4. The calibration results of standard concentrations in the subcatchments of the Gulf of Finland.

Drainage basin	Phosphorus		Nitrogen	
	cO_{forest}	cO_{field}	cO_{forest}	cO_{field}
River Kymijoki	80	300	2 200	8 000
Rest of Finland	80	330	2 200	13 000
Russia	40	130	1 300	2 000
Estonia	40	140	1 300	2 000

Table 5. The annual effects (percentage changes from the present values) of climate change on runoff and nutrient transport. q = runoff, tot-P = total phosphorus transport, tot-N = total nitrogen transport.

Modelling year	q (%)	tot-P (%)	tot-N (%)
2020	+ 2.4	+ 4.3	+ 3.7
2050	+ 4.3	+ 7.5	+ 6.4
2100	+ 7.1	+ 12.4	+ 10.7

Finland were 2–6 times larger than in Russia and Estonia. This is explained by the forestry practices and fertilizer levels in agriculture which are nowadays much lower in Russia and Estonia than in Finland.

At the annual scale the effects of climate change on runoff are quite small (Table 5).

As a result of climate change, the seasonal transport is increased between December and April and decreased between May and August. The situation during other months remains almost unchanged (Fig. 3).

The proportions of the diffuse load of total phosphorus and nitrogen are 15% and 23% of total nutrient, respectively (Tables 2 and 3). Point sources are still the main polluters of the Gulf of Finland, especially in Russia. Thanks to the estimations of bioavailable proportions of total nutrients (see Material and methods) it is possible to present results for dissolved reactive phosphorus (DRP) and dissolved reactive nitrogen (DRN) values in the climate change scenario (Fig. 4).

Temperature model

Initially, water temperature variations in the Gulf of Finland were calculated using meteorological data of the year 1992 (meteorological station of Russärö and wind data from Hanko). There were no water temperature observations available to the authors for this year. The model satisfactorily reproduced the seasonal cycle when compared with mean temperature changes (Mälkki and Tamsalu 1985). Future climate scenarios, generated by GLIGEN, were used to simulate changes in the vertical thermal structure (Fig. 5). Results show that higher rates of air temperature growth cause strong total increase in water temperature as expected. Strong winds lead to high mixing in surface layers, with a deepening of the thermocline by 1–1.5 m and a sharpening of the thermocline zone.

Algal model

The final aim was to characterise the possible effects of the imposed climate change on algal biomass. The evaluation of the calibration simulations was based on two common criteria: the dynamics of
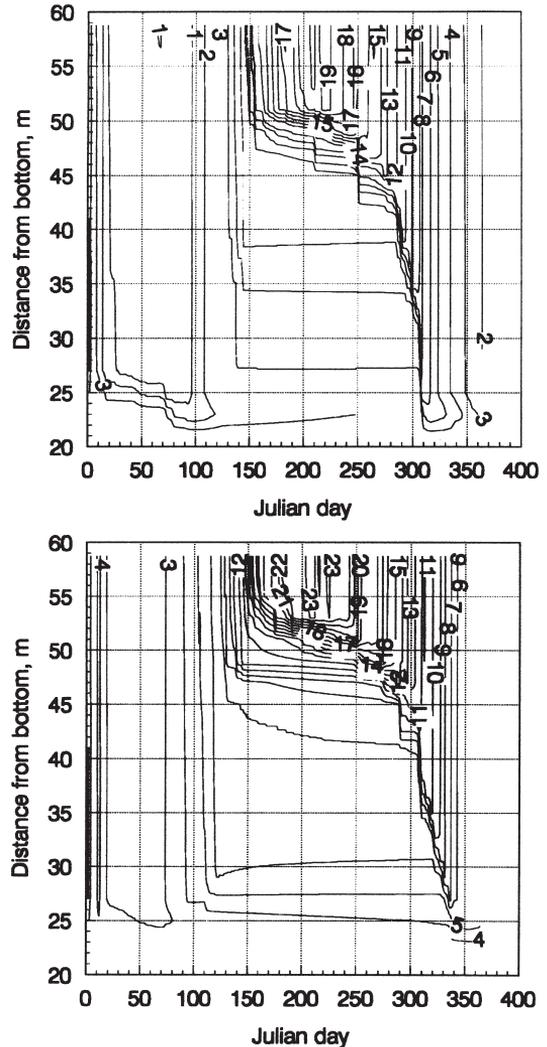
Fig. 5. Two examples of simulations of temperature model. First temperature isophlets are from 2020 central scenario (Carter *et al.* 1995) with 30% increase of strong winds and second one is from 2090 high scenario with 15% increase of strong winds. Time starts from January 1.

phytoplankton and the summer biomass averages. The model was able to describe the two peaks in the concentrations of phytoplankton (Fig 6.), i.e., the higher spring bloom and the lower bloom in late summer.

The average algal biomass concentrations were compared with all measurements of the surface layers of the Gulf of Finland in 1992. Measurements were collected from the database of the

Algal biomass (mg m^{-3})   Chl a (mg m^{-3})
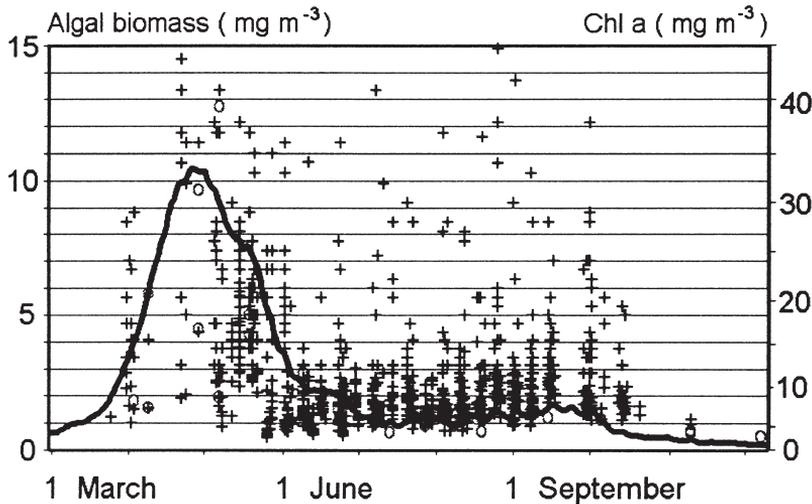
Fig. 6. Time series of horizontally averaged algal biomass concentrations in the surface layer of the Gulf of Finland. Simulation results are compared with all available measurements made in the area in 1992 (measured value of biomass o-mark and chlorophyll *a* +-mark).

Finnish Environment Institute. There were only few measurements of the algal biomass, therefore also chlorophyll-*a* measurements were plotted in Fig. 6. The correlation between algal biomass (c_A) and chlorophyll-*a* (c_{chl}) was calculated by the least square method. All simultaneous biomass and chlorophyll-a measurements from 1990 to 1995 were used. The best correlation ($R^2 = 0.80$) was found with the exponential function (eq. 4; both are in mg m^{-3}).

$$c_A = 149(c_{chl})^{1.211} \qquad (4)$$

The measurements display high variations because the conditions around the various measurement points vari. If these variations are markedly high, there might be blooming in the vicinity. If the variation is relatively low, we can assess the average algal biomass concentration from the measurements.

The conglomeration of measurements (1 June–15 October) and the simulated average algal biomass match quite well. When comparing the simulated average algal biomass concentrations with measurements, one should keep in mind that the major part of measurement points are located in the coastal areas of Finland.

One example of the spatial distribution of the algal biomass is presented in Fig 7. The highest concentrations of algae are found near the load sources and in the coastal area. Upwelling can cause higher algal biomasses in the middle of the Gulf.

The load from St. Petersburg to the Gulf of Finland was kept constant during the simulation period (1 March–11 December) and it was calculated from the annual load averages. The monthly averages were used for riverine loads from the Neva, the Narva and the Kymijoki. The loads of other rivers, municipalities and industry were located evenly along the coastal area. The airborne loads were distributed all over the surface layer and they were calculated by Syri (1996). The atmospheric load for nitrate was 1.089 mg m^{-2} d^{-1} and for ammonium 0.770 mg m^{-2} d^{-1}.

The effect of the three largest rivers (Neva, Narva and Kymijoki) on the Gulf of Finland was simulated. The monthly averages of river flows were used. The wind data used were obtained from the measurement station of Hanko and the same winds were used all over the Gulf of Finland. The flow fields were calculated by Kokkila (Kokkila 1995).

The simulations were performed for three years: 2020, 2050 and 2090. The effect of climate change was described by changes in the temperature regime, river flows and the nutrient loads from the drainage basin.

It was also assumed that the occurrence of strong winds might increase in the future. Three scenarios were used: strong winds (> 7 m s^{-1}) were assumed to increase by 0%, 15% or 30%. Point loads and airborne loads were kept constant in all simulations.

The main conclusions from our results (Fig. 8) are the following. First, the average concentration of phytoplankton will increase only little, because the most important limiting factor is the biologically available nutrients. The loads of bio-

Fig. 7. Simulated algal biomass concentrations at the water surface (0–1 m) in the middle of September 1992.
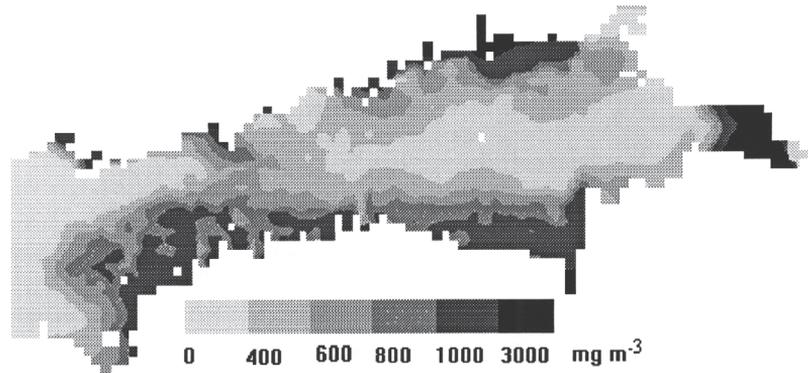
logically available nutrients into the Gulf of Finland will not change much as a consequence of climatic changes, because more than 90% of them originates from industry and municipalities.

Secondly, the average concentration of phytoplankton will be less than 10% higher during the spring bloom in the year 2020. It is possible, that in the year 2090 spring blooms will be about 20% higher than nowadays. The spring blooms will also appear earlier. In the scenarios of the years 2020 and 2050 the temporal changes are only a few days, but in the year 2090 the spring bloom will appear approximately two weeks earlier. Temporal and quantitative changes are caused by faster growth rate of algae, which enable more effective use of nutrients during the spring bloom.

The effect of wind was clear. In the simulations, where the wind velocity distribution is assumed unchanged, the spring bloom is about 10% higher than in the cases where the velocity of wind increases. Strong wind causes higher mixing in surface waters, which decreases surface temperature and transfers algal biomass to deeper layers.

The climate change has it's greatest effect in the Neva estuary (Fig. 9). The spreading of nutrient load from the Neva is smaller due to the earlier spring bloom. Therefore, the effects are relatively smaller in the eastern open sea.

Discussion

The nutrient transport calibration was made by using the annual transport values due to the lack of dynamical data in Estonia and Russia. In the future, it will be possible to perform a dynamical application of the catchment model if the observation practices of meteorological data and water quality parameters are improved.

The effects on runoff are quite small at the annual scale. The increasing evaporation eliminates the effects of the increasing precipitation. The assessed nutrient transport values naturally follow closely the assessed runoff values. The variables that can change nutrient concentrations in this model are the runoff, soil frost and cover type.

The plant cover type in the catchment model (Bilaletdin *et al*. 1996) is the most difficult factor to be estimated for future calculations. Monthly effects of climate change on nutrient transport are slightly slower in the case of the Gulf of Finland than in the inland catchments due to the large catchment areas (Bilaletdin *et al*. 1996).

The effects of the climate change on the algal biomass were rather low in all scenarios, because the most important limiting factor was the nutrients, not the temperature. The uncertainty of the results of the model is linked with the inaccuracy of nutrient availability from the drainage basin, sediment and air.

The results of the temperature model show that in some scenarios the mixed layer can be 1–1.5 meters deeper than nowadays. Therefore changes in the vertically summed algal biomass (mg m^{-2}) can be greater than the modelled changes in the algal biomass concentrations (mg m^{-3}). This is not taken into account in the algal model, where the thickness of layer was 8 meters near the termocline.

Other studies (Kallio *et al*. 1996, Frisk and Bilaletdin 1996 and Saura *et al*. 1996) of the effect of climate change on lakes have been conducted within the SILMU-programme (The Finnish Research Programme on Climate Change). The conclusions of these studies were very similar. The
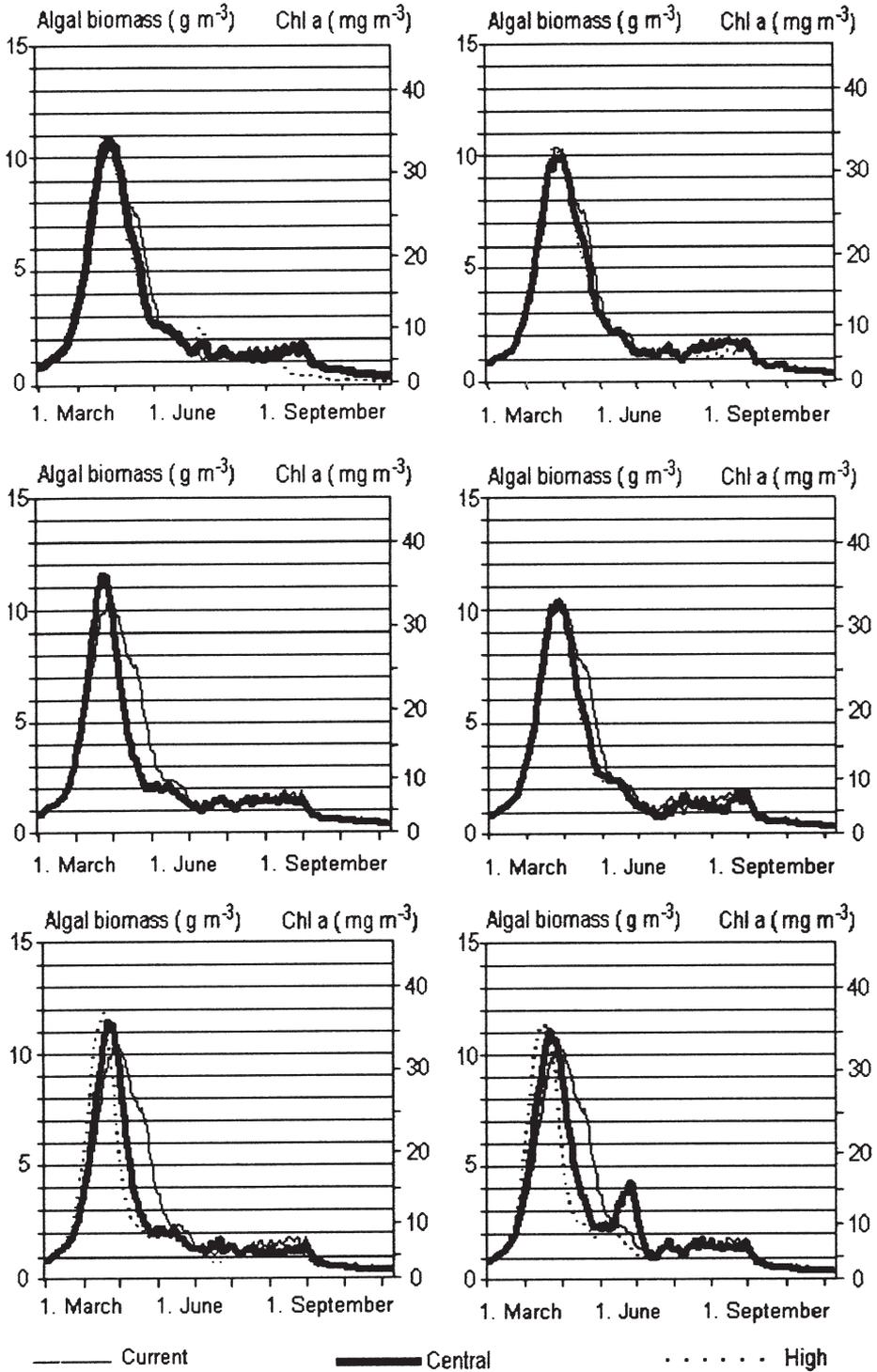
Fig. 8. The effect of climate change on the algal biomass (surface layer average). Top row year 2020, middle 2050 and bottom 2090. Algal biomass is calculated with low, central and high estimate for climate change for each year and compared with the current situation. On the left figures no changes are assumed on wind velocities. Strong winds (> 7 m s⁻¹) are assumed to grow 30% on the right ones.

Fig. 9. The percentual effect of climate change on average algal biomass during 1 March–1 May. Comparison is made between current and 2090 central, no wind increase scenario.
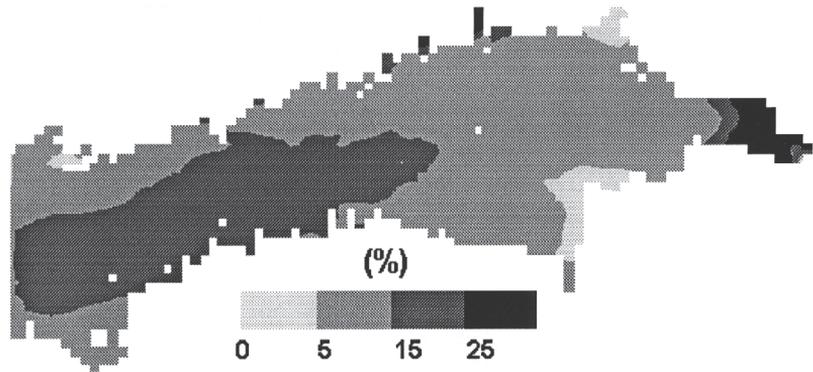
changes in the algal biomass were most extensive during spring bloom (timing and quantity). The changes in the lakes were slightly more extensive than in the Gulf of Finland, because the nutrient loads change more in small catchment areas.

The algal model describes the phytoplankton with only one simulation variable. This includes the assumption that the same species will be dominant in the future. If the distribution of the phytoplankton species change dramatically, also the parameters or even the structure of the model should be different.

The algal model was tried to be kept simple, which made it easier to calibrate. Simplifications can be made, if all main processes are described and they will not change in the future. However, changes in the water temperature can cause surprising effects in the foodweb.

The nutrient loads did not change much in these scenarios, although in practice they can change very much until 2020, 2050 or 2090. The anthropogenic nutrient loads can change considerably regardless of the climate change.

References

Bergström S. 1976. Development and application of a conceptual runoff model for Scandinavian catchments. *SMHI rapporter, RHO* 7, Norrköping. 134 pp.

Bilaletdin Ä., Frisk T., Vehviläinen B., Kallio K., Huttunen M. & Kaipainen H. 1996. Modelling the effects of climate change on nutrient transport from large drainage basins. In: Roos J. (ed.): *The Finnish Research Programme on Climate Change — Final Report*. Publications of the Academy of Finland 4/96, pp. 173–178.

Carter T., Posch M. & Tuomenvirta H. 1995. SILMUSCEN and CLIGEN User's Guide, *Publications of the Academy of Finland* 5/95, 62 pp.

Ehlin U. 1981. Hydrology of the Baltic Sea. In: Voipio, A. (ed.), *The Baltic Sea*, pp. 123–134.

Ekholm P. 1991. Bioavailability of phorphorus in agriculturally loaded rivers in southern Finland. *Hydrobiologia* 287: 179–194.

Frisk T. & Bilaletdin Ä. 1996. Modelling the effects on climate change on eutrophication — the case study of lake Längelmävesi. In: Roos J. (ed.), *The Finnish Research Programme on Climate Change, Final Report*, Publication of the Academy of Finland 4/96, pp. 158–162.

Frisk T. & Nyholm B. 1980. Lämpötilan vaikutuksista reaktionopeuskertoimiin. *Vesitalous* 5: 24–27.

Hansen W. 1956. Theorie zur Errechnung des Wasserstandes und der Strömungen in Randmeeren nebst Anwendungen. *Tellus* 8: 287–300.

Heinonen P. (ed.) 1993. Suomenlahden vesien tilan ja käyttökelpoisuuden valvonta (Suomen osapuolen raportti). Vesi- ja ympäristöhallituksen vesi- ja ympäristöntutkimustoimisto. *Memorandum.* 58 pp.

HELCOM 1991. Interim Report on the State of the Coastal Waters of the Baltic Sea. *Baltic Sea Environment Proceedings* No. 40, 96 pp.

HELCOM 1993. Second Baltic Sea Pollution Load Compilation. Balt. Sea Environ. *Baltic Sea Environment Proceedings.* No. 45, 161 pp.

Inkala A. 1993. Vesistöjen ravintoverkoston 3-dimensioinen laskenta — typen kierto. *Diplomityö*, TKK, Ydin- ja energiatekniikan laitos, Espoo, 62 pp.

Jrgensen S. 1988. *Fundamentals of ecological modelling*, Amsterdam, 391 pp.

Kallio K., Huttula T. & Lehtinen K. 1996. Climate change and the eutrophication of a shallow, agriculturally loaded lake. In: Roos J. (ed.), *The Finnish Research Programme on Climate Change, Final Report*, Publication of the Academy of Finland 4/96, pp. 141–145.

Kokkila T. 1995. Suomenlahden virtausten mallintaminen. *Diplomityö*, TKK, systeemianalyysin laitos, Espoo, 53 pp.

Koponen J., Alasaarela E., Lehtinen K., Sarkkula J., Simbierowicz P., Vepsä H. & Virtanen M. 1992. Modelling the dynamics of a large sea area, *Publications of water and environment research institute* no. 7, 91 pp.

Kullenberg G. 1981. Physical oceanography. In: Voipio, A. (ed.), *The Baltic Sea*, pp. 135–181.

Lehman J., Botkin D. & Likes G. 1975. The assumptions and rationales of a computer model of phytoplankoton population dynamics. *Limnology and Oceanograph* 20: 343–364.

Leppäjärvi R. (ed.) 1992. *Hydrological Yearbook 1989*. National Board of Waters and the Environment. Helsinki. 174 pp.

Lääne A., Loigu E., Kuslap P., Raia T., Puolanne J., Pitkänen H. & Palosaari M. 1991. Pollution load on the Gulf of Finland in 1985–86. A report of studies under the Finnish-Soviet Working Group on the Protection of the Gulf of Finland. *Memorandum*. 18 pp.

Merenkulkuhallitus, 1992, *Merikortti* 901–902, Helsinki, 2 pp.

Pitkänen H. 1994. Eutrophication of the Finnish coastal waters: Origin, fate and effects of riverine nutrient fluxes, *Publications of the Water and Environment Research Institute* no: 18, 45 pp.

Pitkänen H., Kangas P., Sarkkula J., Lepistö L., Hällfors G. & Kauppila P. 1990. Veden laatu ja rehevyys itäisellä Suomenlahdella. *Vesi- ja ympäristöhallitus sarja A* 50,

Helsinki, 137 pp.

Pitkänen H., Tamminen T., Kangas P., Huttula T., Kivi K., Kuosa H., Sarkkula J., Eloheimo K., Kauppila P. & Skakalsky B. 1993. Late summer Trophic Conditions in the North-east Gulf of Finlans and the River Neva Estuary, Baltic Sea, *Estuarine, Coastal and Shelf Science* 37: 453–474.

Rekolainen S., Posch M., Kämäri J. & Ekholm P. 1991. Evaluation of the accuracy and precision of annual phosphorus load estimates from two agricultural basins in Finland. *J. of Hydrology* 128: 237–255.

Saura M., Frisk T., Bilaletdin Ä. & Huttula T. 1996. The effects of climatic change on a small polyhumic lake. In: Roos J. (ed.) *The Finnish Research Programme on Climate Change, Final Report*, Publication of the Academy of Finland 4/96: 163–166.

Scavia D., Eadie B. & Robertson A. 1976. An ecological model for Lake Ontario. Model formulation, calibration and preliminary evaluation NOAA, *Technical report ERL* 371 *GLERL* 12. 63 pp.

Syri S., Johanson M. & Kangas L. 1997. Application of nitrogen transfer matrices for integrated assessment. *Atmospheric Environment*. (In press).

Svensson U. 1978. A mathematical model of seasonal thermocline. Lund Institute of Technology. *Report* No. 1002, Lund, Sweden. 187 pp.

Vehviläinen, B. 1992. Snow cover models in operational watershed forecasting. *Publications of Water and Environment Research Institute* No 11, 112 pp.

Appendices

App. 1. The variables of algal model.

Symbol	Definition	Unit	Symbol	Definition	Unit
c_{Ndet}	Nitrogen in detritus	mg m^{-3}	L_{NH}	Ammonium load	kg d^{-1}
c_{NH}	Ammonium concentration	mg m^{-3}	L_{NO}	Nitrate load	kg d^{-1}
c_{NO}	Nitrate concentration	mg m^{-3}	L_{Pdet}	Detritus phosphorus load	kg d^{-1}
c_{NA}	Nitrogen in algae cells	mg m^{-3}	L_{PO}	Phosphate load	kg d^{-1}
c_{Pdet}	Phosphorus in detritus	mg m^{-3}	t	Time	d
c_{PO}	Phosphate concentration	mg m^{-3}	h	Depth of sell	m
c_{PA}	Phosphorus in algae cells	mg m^{-3}	l	Total irradiance	MJ m^{-2}d^{-1}
c_A	Algae biomass	mg m^{-3}	T	Temperature of layer	°C
L_{Ndet}	Detritus nitrogen load	kg d^{-1}	T_c	Reference temperature	°C

App. 2. The parameters of algal model.

Symbol	Definition	Value	Unit
β_0	detritus nitrogen decay rate	0.018	d^{-1}
v_{Ndet}	settling of detritus nitrogen	4	cm d^{-1}
β_1	nitrification rate	0.15	d^{-1}
D_{NO}	denitrification rate	4	cm d^{-1}
a_{pr}	preference coefficient	1	–
γ_0	detritusphosporus decay rate	0.02	d^{-1}
v_{Pdet}	settling of detritus phosphorus	4	cm d^{-1}
μ_{max}	maximal growth rate of algae	2.5	d^{-1}
K_{P}	half-saturation coefficient of phosphorus uptake of algae	250	mg l^{-1}
K_{N}	half-saturation coefficient of nitrogen uptake of algae	60	mg l^{-1}
$\left(\dfrac{c_{\mathrm{PA}}}{c_{\mathrm{A}}}\right)_{\mathrm{min}}$	minimum phosphorous ratio	0.003	gP gC^{-1}
$\left(\dfrac{c_{\mathrm{PA}}}{c_{\mathrm{A}}}\right)_{\mathrm{max}}$	maximum phosphorous ratio	0.044	gP gC^{-1}
$\left(\dfrac{c_{\mathrm{NA}}}{c_{\mathrm{A}}}\right)_{\mathrm{min}}$	minimum nitrogen ratio	0.05	gN gC^{-1}
$\left(\dfrac{c_{\mathrm{NA}}}{c_{\mathrm{A}}}\right)_{\mathrm{max}}$	maximum nitrogen ratio	0.335	gN gC^{-1}
u_{Pmax}	maximal uptake rate of P	0.243	gP gC^{-1} d^{-1}
u_{Nmax}	maximal uptake rate of N	0.04	gN gC^{-1}d^{-1}
M_{Amax}	maximal decay rate of algae	0.05	d^{-1}
FL	limit value for fast sedimentation	0.06	–
S_{fa}	fast sedimentation acceleration	2.0	–
I_{opt}	optimal radiation	10	MJ m^{-2}

App. 3. Differential equations, rates and limiting factors.

Equations:

$$\frac{\partial c_{\text{Ndet}}}{\partial t} = c_{\text{NA}} M_A - \beta_0 c_{\text{Ndet}} - v_{\text{Ndet}} c_{\text{Ndet}} h^{-1} + L_{\text{Ndet}} \tag{1}$$

$$\frac{\partial c_{\text{NH}}}{\partial t} = -\beta_1 c_{\text{NH}} - u_N \text{FR}_{\text{NH}} - \beta_0 c_{\text{Ndet}} + L_{\text{NH}} \tag{2}$$

$$\frac{\partial c_{\text{NO}}}{\partial t} = \beta_1 c_{\text{NH}} - u_N \text{FR}_{\text{NO}} - c_{\text{NO}} D_{\text{NO}} h^{-1} + L_{\text{NO}} \tag{3}$$

$$\frac{\partial c_{\text{Pdet}}}{\partial t} = c_{\text{PA}} M_A - \gamma_0 c_{\text{Pdet}} - v_{\text{Pdet}} c_{\text{Pdet}} h^{-1} + L_{\text{Pdet}} \tag{4}$$

$$\frac{\partial c_{\text{PO}}}{\partial t} = -u_P + \gamma_0 c_{\text{Pdet}} + L_{\text{PO}} \tag{5}$$

$$\frac{\partial c_{\text{NA}}}{\partial t} = u_N + c_{\text{NA}} M_A \tag{6}$$

$$\frac{\partial c_{\text{PA}}}{\partial t} = u_P + c_{\text{PA}} M_A \tag{7}$$

$$\frac{\partial c_A}{\partial t} = (\mu_A - M_A) C_A \tag{8}$$

Rates:

$$m_A = m_{\max} f_s(c_A, c_{\text{NA}}, c_{\text{PA}}) \, f_I(I) f_T(T) \tag{9}$$

$$M_A = M_{A\max}(f_T(T) + S_{\text{fa}} \text{LIM}) \tag{10}$$

$$\text{LIM} = 0, \text{ when } f_S(c_A, c_{\text{NA}}, c_{\text{PA}}) > \text{FL} \tag{11}$$

$$\text{LIM} = 1, \text{ when } f_S(c_A, c_{\text{NA}}, c_{\text{PA}}) \le \text{FL} \tag{12}$$

$$\text{FR}_{\text{NH}} = \frac{c_{\text{NH}} a_{\text{pr}}}{c_{\text{NH}} a_{\text{pr}} + c_{\text{NO}}} \tag{14}$$

$$u_N = \frac{\left(\frac{c_{\text{NA}}}{c_A}\right)_{\max} - \left(\frac{c_{\text{NA}}}{c_A}\right)}{\left(\frac{c_{\text{NA}}}{c_A}\right)_{\max} - \left(\frac{c_{\text{NA}}}{c_A}\right)_{\min}} \times \frac{u_{\text{Nmax}}(c_{\text{NH}} + c_{\text{NO}})}{K_N + c_{\text{NH}} + c_{\text{NO}}} \times c_A \tag{15}$$

$$u_P = \frac{\left(\frac{c_{\text{PA}}}{c_A}\right)_{\max} - \left(\frac{c_{\text{PA}}}{c_A}\right)}{\left(\frac{c_{\text{PA}}}{c_A}\right)_{\max} - \left(\frac{c_{\text{PA}}}{c_A}\right)_{\min}} \times \frac{u_{\text{Pmax}} c_{\text{PO}}}{K_P + c_{\text{PO}}} \times c_A \tag{16}$$

Limiting factors:

$$f_s(c_A, c_{\text{NA}}, c_{\text{PA}}) = \frac{\left(\frac{c_{\text{PA}}}{c_A}\right) - \left(\frac{c_{\text{PA}}}{c_A}\right)_{\min}}{\left(\frac{c_{\text{PA}}}{c_A}\right)_{\max} - \left(\frac{c_{\text{PA}}}{c_A}\right)_{\min}} \times \frac{\left(\frac{c_{\text{NA}}}{c_A}\right) - \left(\frac{c_{\text{NA}}}{c_A}\right)_{\min}}{\left(\frac{c_{\text{NA}}}{c_A}\right)_{\max} - \left(\frac{c_{\text{NA}}}{c_A}\right)_{\min}} \tag{17}$$

$$f_T(T) = f(T_s) \exp\left[\int_{T_s}^{T} \ln\theta \, dT\right] \tag{18}$$

$$\theta = a + bT \tag{19}$$

$$f(I) = 1, \text{ when } I \ge I_{\text{opt}} \tag{20}$$

$$f(I) = I/I_{\text{opt}}, \text{ when } I < I_{\text{opt}} \tag{21}$$

App. 4. Constants for temperature correction function $q = a + bT$.

symbol definition	a (–)	b ($°C^{-1}$)
μ_{max}: maximal growth rate of algae	1.257	– 0.011
M_{Amax}: maximal decay rate of algae	1.020	– 0.001